1-1-2009

(-)-Epigallocatechin-3-gallate (EGCG) maintains k-casein in its pre-fibrillar state without redirecting its aggregation pathway

Sean A. Hudson
University of Adelaide

Heath Ecroyd
University of Wollongong, heathe@uow.edu.au

Francis C. Dehle
University of Adelaide

Ian F. Musgrave
University of Adelaide

John Carver

(-)-Epigallocatechin-3-gallate (EGCG) maintains k-casein in its pre-fibrillar state without redirecting its aggregation pathway

Abstract

The polyphenol (-)-epigallocatechin-3-gallate (EGCG) has recently attracted much research interest in the field of protein-misfolding diseases because of its potent anti-amyloid activity against amyloid-beta, alpha-synuclein and huntingtin, the amyloid-fibril-forming proteins involved in Alzheimer's, Parkinson's and Huntington's diseases, respectively. EGCG redirects the aggregation of these polypeptides to a disordered off-folding pathway that results in the formation of non-toxic amorphous aggregates. whether this anti-fibril activity is specific to these disease-related target proteins or ismore generic remains to be established. In addition, the mechanism by which EGCG exerts its effects, as with all anti-amyloidogenic polyphenols, remains unclear. To address these aspects, we have investigated the ability of EGCG to inhibit amyloidogenesis of the generic model fibril-forming protein RCMkappa-CN (reduced and carboxymethylated kappa-casein) and thereby protect pheochromocytoma-12 cells from RCMkappa-CN amyloid-induced toxicity. We found that EGCG potently inhibits in vitro fibril formation byRCMkappa-CN [the IC50 for 50 uM RCMkappa-CN is 1 uM]. Biophysical studies reveal that EGCG prevents RCMkappa-CN fibril formation by stabilising RCMkappa-CN in its nativelike state rather than by redirecting its aggregation to the disordered, amorphous aggregation pathway. Thus, while it appears that EGCG is a generic inhibitor of amyloid-fibril formation, the mechanism by which it achieves this inhibition is specific to the target fibril-forming polypeptide. It is proposed that EGCG is directed to the amyloidogenic sheet-turn-sheet motif of monomeric RCMkappa-CN with high affinity by strong non-specific hydrophobic associations. Additional non-covalent pi-pi stacking interactions between the polyphenolic and aromatic residues common to the amyloidogenic sequence are also implicated.

Keywords

egcg, k, casein, its, pre, state, without, redirecting, aggregation, pathway, 3, maintains, fibrillar, gallate, epigallocatechin, CMMB

Disciplines

Life Sciences | Physical Sciences and Mathematics | Social and Behavioral Sciences

Publication Details

Hudson, S. A., Ecroyd, H., Dehle, F. C., Musgrave, I. F. & Carver, J. (2009). (-)-Epigallocatechin-3-gallate (EGCG) maintains k-casein in its pre-fibrillar state without redirecting its aggregation pathway. Journal of Molecular Biology, 392 (3), 689-700.

doi:10.1016/j.jmb.2009.07.031 J. Mol. Biol. (2009) 392, 689–700

JMB

Available online at www.sciencedirect.com

ScienceDirect

ELSEVIER

(–)-Epigallocatechin-3-Gallate (EGCG) Maintains κ-Casein in Its Pre-Fibrillar State without Redirecting Its Aggregation Pathway

Sean A. Hudson[1], Heath Ecroyd[1], Francis C. Dehle[1], Ian F. Musgrave[2] and John A. Carver[1]*

[1]*School of Chemistry & Physics, The University of Adelaide, Adelaide, South Australia 5005, Australia*

[2]*Discipline of Pharmacology, School of Medical Sciences, The University of Adelaide, Adelaide, South Australia 5005, Australia*

Received 22 May 2009; received in revised form 7 July 2009; accepted 9 July 2009
Available online 17 July 2009

The polyphenol (−)-epigallocatechin-3-gallate (EGCG) has recently attracted much research interest in the field of protein-misfolding diseases because of its potent anti-amyloid activity against amyloid-β, α-synuclein and huntingtin, the amyloid-fibril-forming proteins involved in Alzheimer's, Parkinson's and Huntington's diseases, respectively. EGCG redirects the aggregation of these polypeptides to a disordered off-folding pathway that results in the formation of non-toxic amorphous aggregates. Whether this anti-fibril activity is specific to these disease-related target proteins or is more generic remains to be established. In addition, the mechanism by which EGCG exerts its effects, as with all anti-amyloidogenic polyphenols, remains unclear. To address these aspects, we have investigated the ability of EGCG to inhibit amyloidogenesis of the generic model fibril-forming protein RCMκ-CN (reduced and carboxymethylated κ-casein) and thereby protect pheochromocytoma-12 cells from RCMκ-CN amyloid-induced toxicity. We found that EGCG potently inhibits *in vitro* fibril formation by RCMκ-CN [the IC_{50} for 50 μM RCMκ-CN is 13 ± 1 μM]. Biophysical studies reveal that EGCG prevents RCMκ-CN fibril formation by stabilising RCMκ-CN in its native-like state rather than by redirecting its aggregation to the disordered, amorphous aggregation pathway. Thus, while it appears that EGCG is a generic inhibitor of amyloid-fibril formation, the mechanism by which it achieves this inhibition is specific to the target fibril-forming polypeptide. It is proposed that EGCG is directed to the amyloidogenic sheet–turn–sheet motif of monomeric RCMκ-CN with high affinity by strong non-specific hydrophobic associations. Additional non-covalent π–π stacking interactions between the polyphenolic and aromatic residues common to the amyloidogenic sequence are also implicated.

Keywords: amyloid fibril; κ-casein; polyphenol; (−)-epigallocatechin-3-gallate; EGCG

Edited by K. Kuwajima

Introduction

Protein-misfolding diseases encompass over 40 debilitating and incurable human conditions associated with the failure of a specific peptide or protein to adopt or remain in its native functional state.[1] These conditions include pathologies as diverse as Alzheimer's disease, Parkinson's disease, cataract and type II diabetes.[1] The majority of misfolding diseases are associated with amyloidosis.[1,2] This pathological state involves the aggregation of specific polypeptides into highly stable and cytotoxic filamentous deposits known as amyloid fibrils, which comprise a characteristic core of cross-β-sheet

*Corresponding author. E-mail address: john.carver@adelaide.edu.au.

Present address: H. Ecroyd, School of Biological Sciences, University of Wollongong, Wollongong, New South Wales 2522, Australia.

Abbreviations used: BSA, bovine serum albumin; DLS, dynamic light scattering; EGCG, (−)-epigallocatechin-3-gallate; MTT, methylthiazolyldiphenyl-tetrazolium bromide; NBT, nitroblue tetrazolium; PC12, pheochromocytoma-12; RCMκ-CN, reduced and carboxymethylated κ-casein; TEM, transmission electron microscopy; ThT, thioflavin T; TOCSY, total correlated spectroscopy; a.u., arbitrary units.

structure.[1–3] As the number of people suffering from amyloidosis is increasing rapidly in developed countries, due to longer average life expectancies, understanding the aggregation process and knowing how to prevent amyloid-fibril formation have become major challenges.[2]

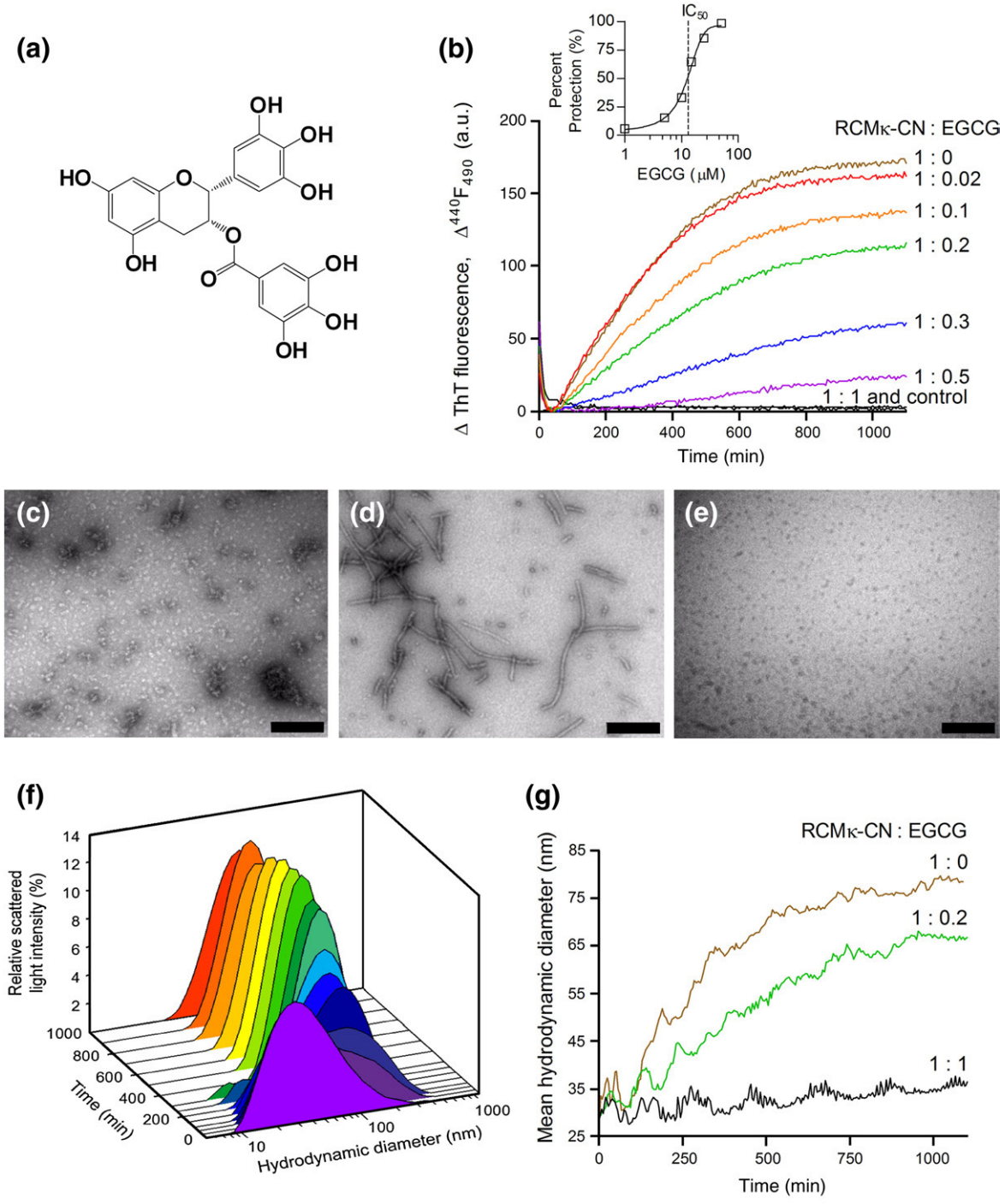

Fig. 1. EGCG inhibits RCMκ-CN amyloid-fibril formation. (a) The structure of the EGCG. (b) *In situ* ThT fluorescence assay of RCMκ-CN (50 μM) incubated at 37 °C in the presence and in the absence of EGCG. A solution of EGCG (50 μM) without RCMκ-CN was also monitored (control). Values shown are the mean readings from three individual experiments, and the standard errors for each data point are within 4% (not visible). Inset plot shows the fitted logarithmic concentration–response (percentage of protection) curve (variable slope model) for calculating the IC_{50}. All percentage-of-protection data points are significantly different ($P<0.05$, one-way ANOVA, Bonferroni's post hoc test, $n=3$). (c–e) TEM micrographs of samples from the *in situ* ThT fluorescence assay: (c) fresh native RCMκ-CN prior to incubation, (d) RCMκ-CN alone after incubation and (e) RCMκ-CN in the presence of EGCG (50 μM) after incubation. Bars represent 200 nm. (f) Time-resolved DLS analysis of RCMκ-CN (50 μM) incubated at 37 °C. The particle diameter-intensity distribution profiles are shown at selected time points. (g) Time-resolved DLS analysis of RCMκ-CN (50 μM) with and without EGCG at 37 °C. The mean hydrodynamic diameter of particles is plotted.

There is currently no approved therapeutic agent directed toward amyloid fibrils or fibril precursors. Yet, over the past 5 years, a wide range of compounds have been found to prevent fibril formation, reverse fibrillation and protect against amyloid-fibril-associated cytotoxicity.[4–11] These compounds target the various stages in the life cycle of an amyloidogenic protein, including stabilising the native state, inhibiting the enzymes that process proteins into amyloidogenic peptides, altering protein synthesis and increasing the clearance of misfolded proteins by stimulating protein quality control systems.[4,5,12] However, most prominent is the development of small-molecule drug candidates, termed anti-aggregates, which selectively interact with the aggregating polypeptides and inhibit or reverse the formation of toxic amyloid fibrils and pre-fibrillar entities.[5,7–10]

Natural polyphenolics comprise over 8000 plant-derived compounds found in high concentrations in wine, tea, spices, berries and a wide variety of other plants.[8] They are characterised by the presence of more than one phenol group per molecule.[8] These compounds constitute one of the most potent classes of anti-aggregation agents known to date.[8–10,13,14] In addition to their anti-amyloidogenic properties, these molecules possess potent anti-oxidant activity and a number of other beneficial health effects, such as anti-carcinogenic, anti-viral and anti-inflammatory properties.[8,15] Recently, (−)-epigallocatechin-3-gallate (EGCG) (Fig. 1a), the most abundant polyphenolic extract from green tea, has been under extensive investigation after emerging evidence suggested that it may improve glucose metabolism, lipid metabolism and endothelial function and reduce the effects of arthritis, neurodegenerative diseases, hypertension, coronary heart disease, obesity, inflammation, cancer and insulin resistance.[15–24] Furthermore, this multifunctional polyphenol drastically reduces cognitive impairment and amyloid deposition in Alzheimer's transgenic mice.[25–27] Biochemical studies indicate that the neuroprotective action of EGCG results from its ability to inhibit protein aggregation, suppress/enhance amyloidogenic/non-amyloidogenic proteolytic processes, scavenge free radicals, chelate iron and co-modulate various other cellular pathways.[28–33] In acting as an anti-aggregate, EGCG efficiently inhibits the amyloid-fibril formation of α-synuclein, amyloid-β and huntingtin, the amyloidogenic proteins involved in Parkinson's, Alzheimer's and Huntington's diseases, respectively.[34,35] EGCG directly binds to the natively unfolded polypeptides and redirects their aggregation down an off-folding pathway, resulting in the formation of unstructured, innocuous and highly stable oligomers.[34,35] However, detailed understanding of the interaction between amyloidogenic polypeptides and EGCG, or any other polyphenols for that matter, remains elusive due to the difficulties associated with biophysical characterisation of non-covalent interactions (especially involving large macromolecular assemblies). Moreover, while the anti-amyloid-fibril activity of EGCG has been shown against some disease-related proteins and peptides, it remains to be established whether this activity is specific to these target proteins or is a more generic action that may have application in the treatment of other amyloid-fibril-associated diseases.

To address these issues, we have investigated the effect of EGCG on RCMκ-CN (reduced and carboxymethylated κ-casein), the non-disease-associated amyloid-fibril-forming protein, with which we have considerable experience. RCMκ-CN serves as an excellent model to study generic aspects of fibril formation and its inhibition as it is easily prepared from the bovine milk protein, κ-casein, and forms amyloid fibrils reproducibly in a short time frame under conditions of physiological temperature and pH and without the need for denaturants.[36,37] The resulting amyloid fibrils are also cytotoxic (F.C.D. *et al.*, unpublished results). Native RCMκ-CN exists in a self-associating equilibrium between monomers and spherical micelle-like oligomers.[38] It is the monomeric species that is believed to account for the highly amyloidogenic nature of RCMκ-CN since, although 'natively disordered' in structure (similar to all caseins), its putative central 'horse-and-rider' conformation contains a large hydrophobic and aromatic-rich repeated sheet–turn–sheet motif that acts as a template to form the fibril core.[36,39,40]

Herein, we show that EGCG is an efficient inhibitor of RCMκ-CN fibril formation and its associated cytotoxicity, suggesting that EGCG has generic anti-aggregation activity. Our biophysical studies indicate that the mechanism by which EGCG inhibits fibril formation by RCMκ-CN is through the constraint of the protein in its native-like state rather than by redirecting its aggregation to the disordered (amorphous) pathway. Thus, our results indicate that the mode by which EGCG exerts its anti-amyloid-fibril activity may vary depending on the target species.

Results

EGCG potently inhibits RCMκ-CN amyloid-fibril formation by maintaining the protein in its native-like state

First, to determine the anti-aggregation efficacy of EGCG toward RCMκ-CN, we performed a standard *in situ* thioflavin T (ThT) fluorescence assay using RCMκ-CN (50 μM) in the presence and in the absence of EGCG (1–100 μM) at 37 °C (Fig. 1b). As we have previously reported, the initial decrease in ThT fluorescence during the first 30 min of incubation is attributable to the samples' warming to the incubation temperature.[36] The ThT fluorescence of RCMκ-CN alone increases rapidly after the equilibration period and reaches a plateau after 800–1000 min, which is indicative of amyloid-fibril formation.[36,37] Incubation of RCMκ-CN with EGCG leads to a concentration-dependent decrease in the ThT fluorescence, with 50 μM EGCG (i.e., a 1:1

molar ratio) yielding complete mitigation. By calculating the percentage of protection from the ThT curve of RCMκ-CN alone and fitting a logarithmic concentration–response curve, the EGCG concentration that gives 50% inhibition of the increase in ThT fluorescence (IC_{50}, value±standard error of fit) was 13±1 μM (Fig. 1b, inset). Furthermore, EGCG incubated alone (Fig. 1b, control) produced no change in ThT fluorescence over the course of incubation, indicating that EGCG is neither inherently amyloidogenic nor likely to interact directly with free solvated ThT.

The morphological effects of EGCG (50 μM) on RCMκ-CN (50 μM) fibril formation were assessed simultaneously by transmission electron microscopy (TEM) (Fig. 1c–e). In agreement with our previous studies, TEM micrographs of RCMκ-CN taken before fibril formation indicate that RCMκ-CN exists initially as globular micelle-like species with a diameter of ~30 nm (Fig. 1c).[37] However, at the plateau region (post-incubation), most available pre-fibrillar entities have been incorporated into mature amyloid fibrils (Fig. 1d). Moreover, in accordance with the ThT assay, the presence of EGCG (at a 1:1 molar ratio) inhibits fibrillation entirely and gives rise to RCMκ-CN species (Fig. 1e) with morphology that is typical of oligomers and early pre-fibrillar assemblies (F.C.D. *et al.*, unpublished observations).

To corroborate the findings of the ThT and TEM experiments, we monitored RCMκ-CN (50 μM) fibril formation at 37 °C in the presence and in the absence of EGCG (10 and 50 μM) directly by dynamic light scattering (DLS) (Fig. 1f and g). DLS allows the hydrodynamic diameter of particles in solution to be measured.[41] The particle diameter distribution of RCMκ-CN alone shifts from a peak centred at ~30 nm to ~75 nm over the period of incubation (Fig. 1f). This growth, shown in real time by mean hydrodynamic diameter measurements (Fig. 1g), has dynamics similar to that of the *in situ* ThT data and implies that both the ThT assay and the DLS techniques are monitoring the same aggregation processes. Furthermore, akin to the ThT binding assay, particle growth in the presence of EGCG is suppressed by 20% and 100% at 1:0.2 and 1:1 RCMκ-CN:EGCG molar ratios, respectively.

Therefore, on the basis of the ThT, TEM and DLS analyses, it appears that EGCG mitigates RCMκ-CN amyloidogenesis by constraining the protein in its micellar native-like state, constituting species such as monomers, oligomers and early pre-fibrillar intermediates. Furthermore, assuming a direct RCMκ-CN–EGCG interaction, and since RCMκ-CN fibrillation is prevented so efficiently by EGCG (e.g., ~85% inhibition at 1:0.5 RCMκ-CN/EGCG), it is plausible that a single EGCG molecule interacts with multiple RCMκ-CN species concurrently and that RCMκ-CN has multiple sites for EGCG interaction.

EGCG binds strongly to RCMκ-CN via intermolecular hydrophobic interactions

Proteins that have been separated by SDS-PAGE and electroblotted onto nitrocellulose or polyvinylidene fluoride membrane can be selectively stained with nitroblue tetrazolium (NBT) to identify protein-bound quinone and quinonoid-related substances, such as polyphenols.[34,42,43] Here, we employed this technique to investigate the binding action and selectivity of EGCG. Samples of freshly prepared native RCMκ-CN (50 μM) and bovine serum albumin (BSA) (10 μM) in the presence and in the absence of EGCG (10–100 μM) were separated by SDS-PAGE (Fig. 2a). BSA was used as a standard hydrophobic test protein.[34] The bands were then electroblotted onto polyvinylidene fluoride membrane and stained with NBT (Fig. 2b). The presence of EGCG does not affect electrophoretic migration,

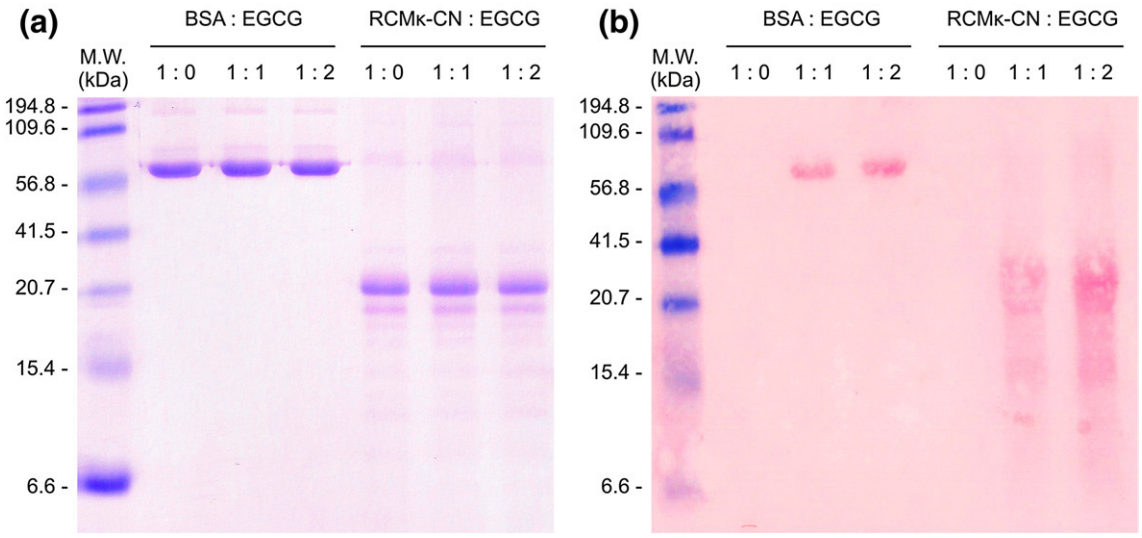

Fig. 2. EGCG binds to BSA and RCMκ-CN. (a) SDS-PAGE analysis of BSA (10 μM) or native RCMκ-CN (50 μM) in the presence and in the absence of EGCG. Ratios above the lanes indicate the molar ratio between protein and EGCG for each sample. The weak bands represent minor protein impurities and are not a result of adding EGCG. (b) NBT staining assay of electroblotted polyvinylidene fluoride membrane of (a).

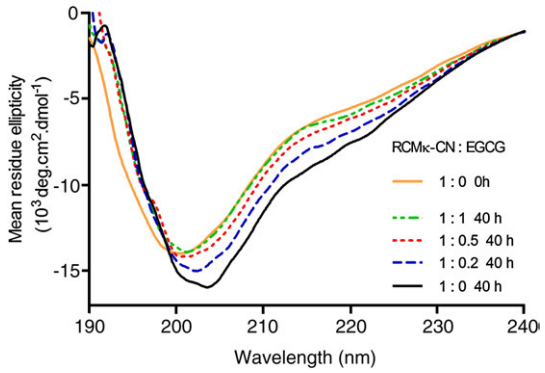

Fig. 3. The changes in secondary structure of RCMκ-CN are prevented by EGCG. Far-UV CD spectra of RCMκ-CN (10 μM) before incubation (0 h) and following incubation at 37 °C for 40 h in the presence and in the absence of EGCG.

and the major protein bands appear at their expected positions (i.e., ~66 and ~19 kDa for BSA and RCMκ-CN, respectively).[34,36,44] The NBT colour reaction occurs for all protein bands from samples containing EGCG. Colorimetric image analysis shows that there is a 1.4-fold increase in formazan stain intensity between the bands of 1:1 and 1:2 protein/EGCG. From these data, it is concluded that EGCG potentially binds to more than one site on each of the proteins. The EGCG–protein association is also sufficiently strong to survive the reducing and denaturing conditions of SDS-PAGE. Moreover, in view of the common hydrophobicity of BSA, RCMκ-CN and EGCG,[37,40,44–48] and since the hydrophobic regions of proteins are readily exposed under SDS-PAGE conditions,[49] these results suggest that a non-specific non-covalent hydrophobic interaction mediates EGCG binding to these proteins.

EGCG prevents the time-dependent changes in the secondary structure of RCMκ-CN

Circular dichroism (CD) spectroscopy was employed to investigate the effect of EGCG binding on RCMκ-CN secondary structure. The far-UV CD spectra of RCMκ-CN (10 μM) with and without EGCG (2–10 μM) were acquired before and after incubation at 37 °C for 40 h to allow for fibril formation and the inhibition thereof (Fig. 3). Native RCMκ-CN alone gives a spectrum with a maximum negative mean residue ellipticity at 200 nm and a shoulder between 213 and 230 nm, which is indicative of a predominantly random coil structure and is in accordance with the CD spectra of RCMκ-CN reported previously.[36,40] Following incubation, the maximum negative mean residue ellipticity at

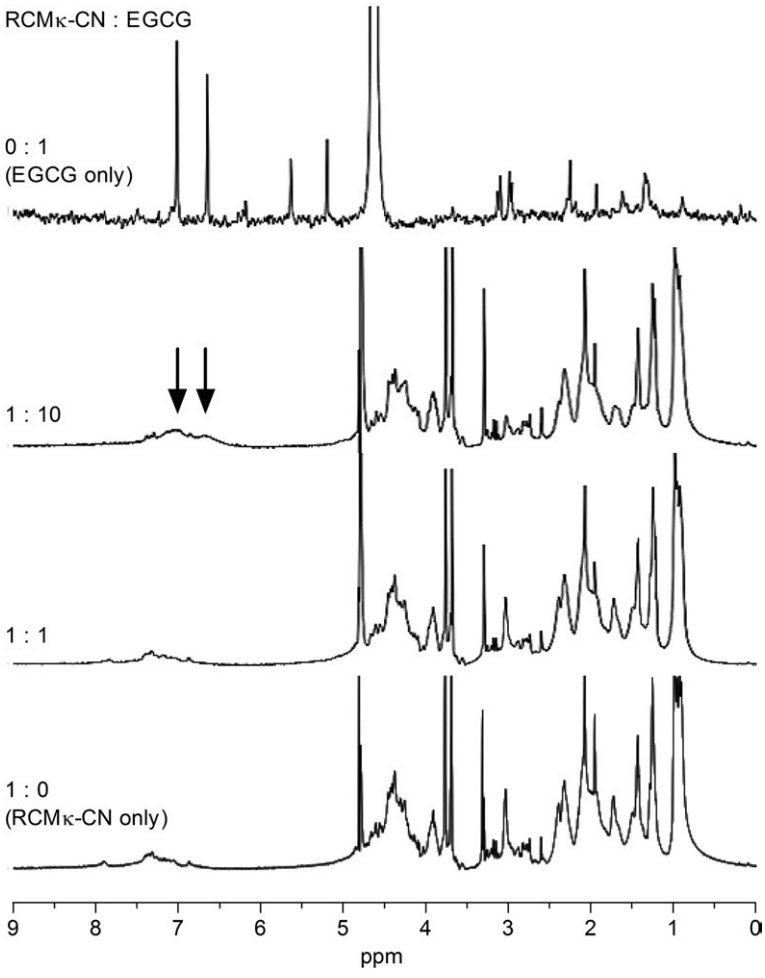

Fig. 4. EGCG interacts with the inflexible regions of RCMκ-CN. One-dimensional ^{1}H NMR spectra of fresh native RCMκ-CN (250 μM) in deuterated sodium phosphate buffer (50 mM, pH 7.4) with and without EGCG recorded at 25 °C. The comparative EGCG (50 μM) spectrum is also shown. The few sharp resonances in the RCMκ-CN spectra (at ~2.0, 3.3 and 3.7 ppm) arise from low-molecular-weight impurities. In the presence of RCMκ-CN, the aromatic resonances of EGCG (at 6.7 and 7.0 ppm, arrows) are only just observed with 10-fold molar excess of EGCG. Resonance intensities for each spectrum are not relative.

200 nm is increased and red-shifted to 204 nm and the shoulder between 213 and 230 nm is also increased in negative ellipticity, in agreement with our previous findings.[36] These changes are indicative of a small loss of random coil and an increase in β-sheet content, which are consistent with the proposal that RCMκ-CN exists with well-positioned β-sheet backbone and thus requires little conformational change to aggregate.[36,40] In the presence of EGCG, the generation of β-sheet that accompanies RCMκ-CN fibril formation is suppressed and RCMκ-CN seemingly does not undergo any changes in secondary structure (Fig. 3). This effect is concentration dependent in accordance with the anti-aggregation efficacy of EGCG (Fig. 1b, inset). Thus, these findings corroborate the evidence that EGCG inhibits the aggregation pathway by stabilising RCMκ-CN in its native-like state.

EGCG interacts with inflexible regions of RCMκ-CN with high affinity as monitored by ^{1}H NMR spectroscopy

To further elucidate the non-covalent binding action of EGCG, we recorded one-dimensional ^{1}H and two-dimensional total correlated spectroscopy (TOCSY) NMR spectra of freshly prepared native RCMκ-CN (250 μM) with and without EGCG (250 and 2500 μM) (Fig. 4; representative and non-redundant TOCSY spectra are presented in the Supplementary Material). The corresponding NMR spectra of EGCG alone (50 μM) were also acquired (Fig. 4). The extensive overlap and lack of chemical shift dispersion of RCMκ-CN NMR resonances are consistent with the relatively unstructured and highly flexible nature of RCMκ-CN.[36,39,40] Titration of RCMκ-CN with equimolar or 10-fold molar excess of EGCG does not lead to the loss or shift of the observed RCMκ-CN resonances or cross-peaks, implying that the conformational flexibility of RCMκ-CN is maintained upon interaction with EGCG and that EGCG does not interact significantly with the flexible regions of RCMκ-CN. Furthermore, since the inflexible (more rigid) regions of monomeric RCMκ-CN are proposed to encompass the highly amyloidogenic sheet–turn–sheet motif,[36,40] EGCG may be directly targeting the amyloidogenic sequence of RCMκ-CN.

The EGCG resonances are broadened significantly when EGCG is in the presence of RCMκ-CN. Even at a 10-fold molar excess, the intense aromatic resonances of EGCG (at 6.7 and 7.0 ppm in the one-dimensional ^{1}H NMR spectrum) are only just observed (Fig. 4). This finding affirms that EGCG is likely to interact with the more rigid regions of RCMκ-CN, thereby increasing its overall correlation time such that its resonances broaden out. Moreover, this observation suggests that EGCG has a high affinity for RCMκ-CN (i.e., resonances of EGCG are not observed because most EGCG is bound to RCMκ-CN). Alternatively, the association–dissociation exchange rate may be intermediate on the NMR timescale, and thus the observed EGCG resonances are broadened out due to a combination of broad and sharp resonances, corresponding to EGCG bound to and that unbound to RCMκ-CN, respectively.

In a second experiment, one-dimensional ^{1}H and two-dimensional TOCSY NMR spectra of RCMκ-CN (250 μM) with and without EGCG (250 and 2500 μM) were recorded after the reaction mixtures had been incubated at 37 °C for 20 h. For all samples, there was no significant difference from the comparable spectra acquired prior to incubation under the fibril-forming conditions (Fig. 4; representative TOCSY data in the Supplementary Material). This implies that there is little structural reconfiguration when RCMκ-CN is sequestered into amyloid fibrils. The flexible regions of RCMκ-CN are thus maintained and must remain exterior to the rigid internal cross-β-sheet amyloid core. We have observed similar behaviour during fibril formation by the small heat-shock protein, αB-crystallin, whereby the C-terminal extension of the protein remains flexible,

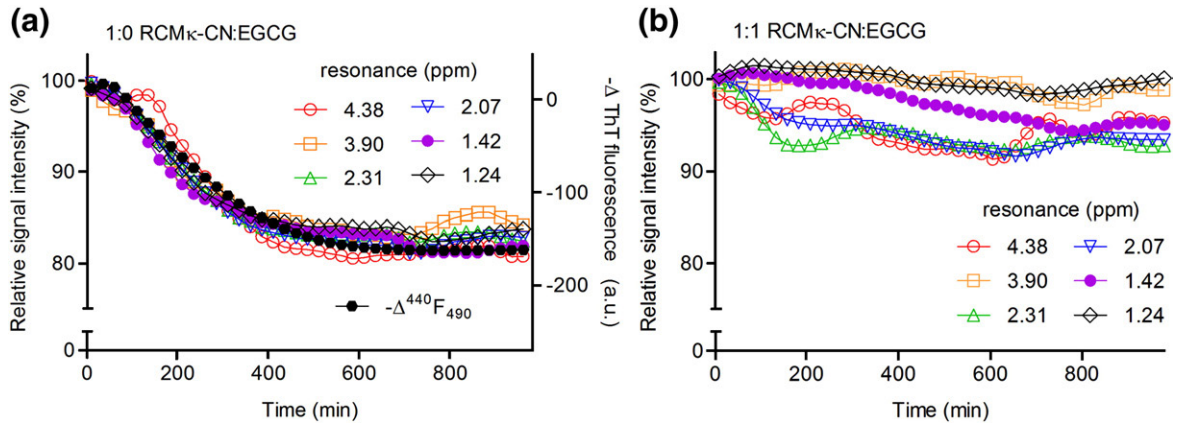

Fig. 5. The real-time interaction between RCMκ-CN and EGCG by NMR spectroscopy. (a and b) The change in intensity of various resonances from real-time ^{1}H NMR spectra acquired every 5 min for samples of RCMκ-CN (50 μM) in deuterated sodium phosphate buffer (50 mM, pH 7.4) incubated at 37 °C in the absence (a) and in the presence (b) of EGCG (50 μM). The negative change in ThT fluorescence of RCMκ-CN (50 μM) is overlaid on (a) to show matching trends between the resonance decay and fibril growth. All profiles of intensity for each sample are not statistically different.

protruding from the fibrillar core.[50] This finding is consistent with the evidence that RCMκ-CN fibril formation occurs through simple sequestration and stacking of the structurally constrained β-sheet region of monomeric RCMκ-CN, with little conformational change necessary to facilitate amyloidogenesis.[36,40] However, over the period of incubation, there is a small decrease in resonance intensity of all RCMκ-CN resonances in the absence of EGCG, as discussed below.

Real-time NMR spectroscopy of the interaction between EGCG and RCMκ-CN

The subtle changes in resonance intensities of the RCMκ-CN ^{1}H NMR resonances were monitored by real-time ^{1}H NMR spectroscopy. Samples of RCMκ-CN (50 μM) with and without EGCG (50 μM) were incubated at 37 °C, one-dimensional ^{1}H NMR spectra were acquired every 5 min and the change in resonance intensity with time was determined (Fig. 5). For RCMκ-CN alone, all resonance decay profiles are essentially identical and occur with the same time constant as the change in ThT fluorescence associated with the formation of amyloid fibrils (Fig. 5a), which implies that they are monitoring the same process. The loss of resonance intensity of the observed flexible RCMκ-CN resonances is consistent with a loss of their conformational flexibility. However, the loss of flexibility is small and uniform (i.e., it is not selective for any particular resonances), corroborating that the mobile regions of RCMκ-CN retain their highly flexible nature in the amyloid structure and that the loss of resonance intensity results primarily from the incorporation of RCMκ-CN into slow-tumbling high-molecular-weight fibrillar assemblies. Interestingly, during the first 60 min of incubation, the loss of resonance intensity is small and is similar to the lag time observed in the overlaid ThT experiment. This period most likely corresponds to the initial period of fibrillation, where RCMκ-CN is aggregating to form small non-fibrillar species, such as oligomers, nuclei and protofibrils, which are not large enough to cause an observable loss in resonance intensity.

In the presence of EGCG, the relative resonance intensities remain mostly unaltered over the period of incubation (Fig. 5b), indicating that amyloidogenesis and the corresponding loss of flexibility of RCMκ-CN are prevented by EGCG and that the interaction of EGCG with RCMκ-CN occurs early along the latter's aggregation profile. Furthermore, this result is consistent with the evidence that EGCG suppresses RCMκ-CN fibril formation by interacting with the inflexible amyloidogenic β-sheet region of RCMκ-CN and thereby keeps RCMκ-CN in its native-like non-fibrillar state.

EGCG protects against RCMκ-CN amyloid-induced cytotoxicity

Finally, to assess the cytoprotective capacity of EGCG, we treated pheochromocytoma-12 (PC12) cells with RCMκ-CN pre-incubated at 37 °C for 20 h with and without EGCG from the *in situ* ThT fluorescence assay (see Fig. 1b). The final concentration of RCMκ-CN was 0.5 μM. Following incubation of the treated cells for 48 h, cellular survival was measured by methylthiazolyldiphenyl-tetrazolium bromide (MTT) reduction (Fig. 6). Treatment with EGCG alone does not affect cell survival. Significant protection from amyloid-associated toxicity is observed when EGCG is present at concentrations higher than 0.05 μM. The effective EGCG concentration that gives 50% cytoprotection (EC_{50}, value± standard error of fit) is 0.17±0.05 μM. Accounting for the 1/100 dilution of the samples when adding them to the cell culture medium, this value is in excellent agreement with the IC_{50} for the inhibition of RCMκ-CN fibril formation by EGCG *in vitro* as determined by ThT fluorescence (i.e., 13±1 μM) (Fig. 1b). Hence, these data indicate that the suppression of RCMκ-CN fibril formation by EGCG *in vitro* results in direct attenuation of its cytotoxic effects.

Discussion

In this study, we have investigated the effect of EGCG on the model non-disease-related amyloidogenic protein, RCMκ-CN, to determine whether EGCG is a generic inhibitor of amyloid-fibril formation and to establish the mechanism by which this inhibition occurs. We have previously shown that RCMκ-CN fibril formation occurs through a unique

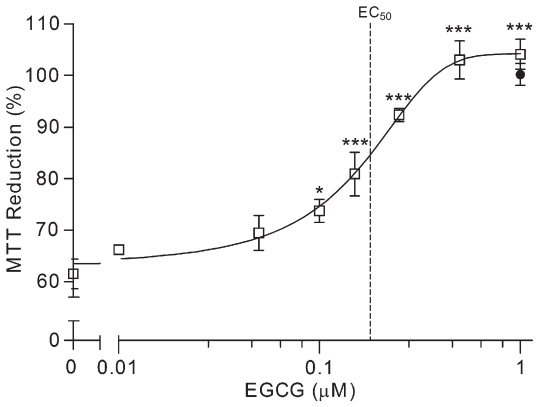

Fig. 6. EGCG protects against cell death by preventing the formation of RCMκ-CN amyloid fibrils. MTT cell survival assay of PC12 cells treated with RCMκ-CN pre-incubated at 37 °C for 20 h in the presence and in the absence of EGCG from the *in situ* ThT assay (see Fig. 1b). The final concentration of RCMκ-CN was 0.5 μM, and that of EGCG was as indicated. Treatment with EGCG alone did not affect cellular survival [filled circle data point shows representative control treatment with EGCG (1 μM) alone]. A sigmoidal logarithmic concentration–response curve (variable slope model) is fitted for calculating the EC_{50}. Values represent mean±SEM ($n=3$). $^*P<0.05$ and $^{***}P<0.001$ *versus* treatment with pre-incubated RCMκ-CN alone (one-way repeated-measures ANOVA, Dunnett's post hoc test). Error bars are not visible when the standard error is less than 1%.

mechanism whereby the rate-limiting step is not a typical nucleation event and rather the dissociation of non-amyloidogenic micelle-like RCMκ-CN oligomers into highly amyloidogenic RCMκ-CN monomers.[36] Energy-minimisation-based-modelling of monomeric RCMκ-CN indicates that, although predominantly unfolded, the monomer can adopt a 'horse-and-rider' conformation that contains a large hydrophobic and aromatic-rich sheet–turn–sheet motif.[39,40] The highly amyloidogenic nature of RCMκ-CN is imputed to this constrained antiparallel β-sheet region since it requires little conformational change to aggregate and forms the cross-β-sheet core of mature RCMκ-CN amyloid fibrils.[36] Moreover, the RCMκ-CN aggregation cascade is proposed to occur through the simple fibrillar alignment and stacking of these well-positioned β-sheet regions.[36,40]

Here, the coupled findings of ThT, TEM, DLS, CD and real-time NMR experiments reveal that EGCG prevents RCMκ-CN fibrillation by binding to and stabilising RCMκ-CN in a native-like state with size, morphology, conformation and flexibility similar to those of native RCMκ-CN, which is incapable of forming amyloid fibrils (Figs. 1, 3 and 5). The inhibition is extremely efficient, with the IC_{50} for RCMκ-CN (50 μM) fibril formation, as assessed by ThT fluorescence, being 13±1 μM (Fig. 1b, inset). Our results indicate that the stabilising action of EGCG does not significantly modify the structure of the RCMκ-CN species and that neither does it redirect RCMκ-CN aggregation down the alternative disordered (amorphous) aggregation pathway. This is in stark contrast to the action of EGCG toward α-synuclein and amyloid-β, where EGCG redirects the aggregation of these polypeptides down an off-folding pathway, resulting in the formation of large SDS-stable amorphous structures.[34] This action is akin to the behaviour we have observed for chaperone proteins, such as αB-crystallin, which redirect α-synuclein from the fibril to the amorphous aggregation pathway.[51,52] Thus, while it appears that EGCG is a generic inhibitor of fibril formation, the mechanism by which it achieves this inhibition is not generic—that is, the nature of the target polypeptide and its mechanism of fibril formation play an important role on the resulting effect of EGCG.

Current understanding of the non-covalent interactions between amyloidogenic polypeptides and EGCG (or other polyphenolics) is based primarily on examination of the physicochemical properties and structural similarities of polyphenols. It is conjectured that polyphenols associate with amyloidogenic sequences of fibril-forming proteins predominantly via a combination of (1) aromatic π–π stacking interactions between the polyphenolic rings and the aromatic residues common to most amyloidogenic sequences, (2) hydrogen bonding to the polypeptide main chain via the phenolic hydroxyls and (3) hydrophobic interactions owing to the lipophilic nature of polyphenols and the inherent hydrophobicity of amyloidogenic sequences.[8,53–55] On interacting, polyphenols are thought to prevent the β-strand/sheet formation and stacking events necessary for fibrillation.[8,54,55] This is achieved by disrupting the hydrogen-bonding network of the β-sheets, the side-chain π-π stacking within the core amyloidogenic sequence and the inherent hydrophobic interactions that are believed to drive aggregation by providing stability, directionality and orientation for self-assembly.[8,53–55] The data presented here add support for these mechanistic theories—that is, the NMR spectroscopy and NBT staining experiments demonstrate that EGCG has a high affinity for the constrained amyloidogenic β-sheet structure of RCMκ-CN through strong SDS-stable hydrophobic associations (Figs. 2 and 4). Moreover, since over 85% of all the aromatic side chains of RCMκ-CN reside within its fibril core (the putative sheet–turn–sheet motif),[36,40] it is likely that π–π stacking interactions are also of importance. It is worth noting that both BSA and RCMκ-CN bind EGCG as monitored using the NBT-based assay (Fig. 2). This is contrary to findings in the study by Ehrnhoefer *et al*.,[34] where EGCG was found to bind urea-denatured BSA but not the untreated protein, and it was speculated that the unfolding of polypeptide chains is a prerequisite for EGCG binding. The poorer sensitivity of the NBT assay in the Ehrnhoefer *et al*. study may account for the discrepancy with our results.

Amyloid deposits are firmly linked with disease, but the mechanisms by which the fibrillar entities lead to cell death are largely unclear.[1,2,56] For years, it was postulated that the insoluble plaques of amyloid fibrils were the most cytotoxic amyloidogenic species (the amyloid hypothesis).[1,56,57] However, recently, this hypothesis has been challenged and there is much debate as to whether the soluble pre-fibrillar intermediates in the typical aggregation pathway are more cytotoxic than the insoluble mature fibrils.[1,58] For instance, there is strong evidence that soluble amyloid-β dimers are the dominant contributors to Alzheimer's disease pathophysiology.[58] Since an anti-aggregate, such as EGCG, is likely to act at multiple steps along the fibril-forming pathway, a concern is that these inhibitors may block the aggregation process and cause the build-up of the cytotoxic pre-fibrillar oligomers, thereby exacerbating the problem. Here, PC12 cell survival studies to assess the protective potential of EGCG reveal that the attenuation of RCMκ-CN fibril formation *in vitro* directly correlates with protection from RCMκ-CN amyloid-induced toxicity (Fig. 6). It is concluded that the primary mechanism by which EGCG affords cytoprotection is via suppression of RCMκ-CN aggregation. However, the known beneficial properties of polyphenols, such as radical scavenging, reduction of reactive oxidative species and/or chelating of metal ions, may also contribute to the amelioration of RCMκ-CN fibril-associated toxicity.[8,15,24,55] Moreover, from the standpoint that EGCG constrains RCMκ-CN in its native-like state, the data imply that mature RCMκ-CN amyloid fibrils are more cytotoxic than their non-fibrillar counterparts. These

data are consistent with our recent studies characterising RCMκ-CN cytotoxicity (F.C.D. *et al.*, unpublished results).

In all, the high efficacy of EGCG as a generic anti-aggregate makes it an excellent candidate for the design and synthesis of more potent fibrillation blockers. Synthesis of EGCG analogues (e.g., via combinatorial chemistry) may provide the answer to its structure–activity relationship and its greater potency over other anti-amyloidogenic polyphenols.[8,13,14,34] Moreover, analogues may be the solution to the challenges of stability, bioavailability and metabolic transformation that face the development of green tea polyphenols as therapeutic agents.[46] Although EGCG was unable to act as a β-sheet breaker (data not shown), the ability of future anti-aggregates to disrupt and destroy preformed amyloid fibrils, and thus reverse the fibrillation pathway, is an important goal. Overall, this work confirms that small-molecule anti-aggregates are an exciting therapeutic strategy for the treatment of amyloidosis and that EGCG, in particular, presents a promising way forward in this endeavour.

Materials and Methods

Materials

Unless specified, all materials and reagents were of analytical grade and obtained from the Sigma Chemical Company (St. Louis, MO, USA). κ-Casein was reduced and carboxymethylated as described by Shechter *et al.*,[59] and the lyophilised RCMκ-CN was stored at −20 °C until use. Black μClear 96-microwell plates were supplied by Greiner Bio-One (Stonehouse, UK), and Thin Seal self-adhesive plate covers were purchased from Excel Scientific (Chicago, IL, USA). Carbon-coated 400-mesh nickel TEM grids were purchased from SPI Supplies (West Chester, PA, USA), and uranyl acetate was bought from Agar Scientific (Stansted, UK). Serum-free medium (RPMI 1640) powder, foetal bovine serum, horse serum and L-glutamine were supplied by Thermo Electron Corporation (Melbourne, Australia). PC12 cells were donated by Prof. John Piletz (University of Mississippi, Oxford, MS, USA). All buffers were filtered using a 0.2-μm syringe filter before use.

Preparation of samples for assay

Unless stated otherwise, all solutions of protein or EGCG and reaction mixtures of EGCG and protein were prepared in sodium phosphate buffer (50 mM, pH 7.4) at 4 °C. For aggregation mixtures, separate solutions of native protein and EGCG were first prepared at twice the required concentration. These stocks were then combined in equal volumes to give the desired molar ratio of protein to EGCG (as indicated in each figure). The desired concentration of native protein solution was achieved by standard spectrophotometric methodology using a CARY 5000 UV-Vis-NIR spectrophotometer (Varian, Melbourne, Australia) and molar extinction coefficients of 0.95 and 0.66 mL mg^{-1} cm^{-1} at 280 nm for RCMκ-CN and BSA, respectively.[60,61] Once prepared, samples were then used immediately in assay or pre-incubated at 37 °C for 20 or 40 h (as indicated in each figure) to allow for the formation of RCMκ-CN amyloid fibrils or inhibition thereof by EGCG.

In situ thioflavin T fluorescence assay

ThT (10 μM) was added to 200-μL samples using a stock ThT solution (200 μM) prepared in filtered sodium phosphate buffer (50 mM, pH 7.4). The samples were then incubated at 37 °C in black μClear 96-microwell plates that were sealed to prevent evaporation. The ThT fluorescence intensity of each sample was recorded every 5 min using a FLUOstar OPTIMA plate reader (BMG Labtechnologies, Melbourne, Australia) with 440-/490-nm excitation/emission filters set. Since native RCMκ-CN binds some ThT due to its β-sheet content,[40] the ThT data were normalised by plotting the change in ThT fluorescence [arbitrary units (a.u.)], ΔF, as determined by the following equation: $\Delta F = F - F_{30}$, where F is the mean ThT fluorescence reading (a.u.) from triplicate experiments and F_{30} is the mean ThT fluorescence reading (a.u.) after 30 min of incubation once all samples had evenly equilibrated to 37 °C. The percentage of protection (%) was calculated using the following equation: Percent Protection = $[1 - \Delta F_{30}(\text{RCM}\kappa\text{-CN} + \text{EGCG}) / \Delta F_{30}(\text{RCM}\kappa\text{-CN})] \times 100$, where $\Delta F_{30}(\text{RCM}\kappa\text{-CN} + \text{EGCG})$ is the mean change in ThT fluorescence measurement (a.u.) at the plateau phase for samples of RCMκ-CN treated with EGCG and $\Delta F_{30}(\text{RCM}\kappa\text{-CN})$ is the mean change in ThT fluorescence measurement (a.u.) for the control sample of RCMκ-CN alone at the plateau phase. The presence of ThT at the concentration used did not affect RCMκ-CN fibril formation.[37] EGCG is not spectroscopically active at the wavelengths of ThT fluorescence and does not influence the detected ThT fluorescence (data not shown).

Transmission electron microscopy

Two-microliter aliquots were taken from samples of the ThT fluorescence assay before or after incubation (as indicated in each figure) and transferred onto the surface of carbon-coated 400-mesh nickel TEM grids. The grid surface was then washed with 0.22-μm filtered MilliQ water (3×10 μL) and negatively stained with uranyl acetate solution (10 μL, 2% w/v, in MilliQ). Between each wash and after staining, excess solution was removed by absorbing with filter paper. The grid was left to air dry and then viewed under magnification of 25,000×–64,000× using a Philips CM100 transmission electron microscope (Philips, Eindhoven, The Netherlands) with an 80-kV excitation voltage.

Dynamic light scattering

Time-resolved DLS analysis was performed at 37 °C using a Zetasizer Nano-ZS (Malvern Instruments, Worcestershire, UK). Every 5 min, the particle diameter-intensity distribution and mean hydrodynamic diameter were determined from 13 acquired correllograms using the program CONTIN[62] and the method of cumulants,[63] respectively, via the attached Dispersion Technology Software (Malvern Instruments Ltd., Worcestershire, UK).

Nitroblue tetrazolium staining

NBT staining of proteins electroblotted onto 0.2-μm polyvinylidene fluoride membrane was performed as

described previously.[34,42] The intensity of formazan bound to each band was quantified using gel colorimetric imaging analysis in ImageJ 1.40g software (Wayne Rasband, National Institute of Health, MD, USA).

Circular dichroism spectroscopy

Far-UV CD spectra were recorded at 37 °C on a JASCO J-815 CD spectropolarimeter (JASCO, Easton, MD, USA) using a 0.1-cm path-length cuvette and a step of 0.1 nm, a scan rate of 20 nm s^{-1}, 4 s of delay and a scan average of five. The acquired spectra were corrected for minor solvent or EGCG contributions by subtracting the reference spectra of buffer or corresponding EGCG solution without RCMκ-CN. The far-UV CD spectra of all samples prior to incubation were identical (data not shown).

Solution-state ^{1}H NMR spectroscopy

Samples were prepared as described above with the exception that filtered sodium phosphate buffer (50 mM, pH 7.4) was prepared using deuterium oxide in place of MilliQ water. Samples were placed in separate 535-PP NMR tubes (Wilmad, Buena, NJ, USA), and one-dimensional ^{1}H and two-dimensional TOCSY spectra were acquired using a Varian UNITY Inova NMR spectrometer (Varian, Palo Alto, CA, USA) equipped with an Oxford 600 MHz magnet (Oxford, UK) and a pulse-field gradient 5-mm probe. The spectrometer was operated at 600 MHz with a sweep width of 7000.5 Hz and a relaxation delay of 1 s, and water signal suppression was achieved using a PRESAT pulse sequence. Single spectra were recorded at 25 °C to prevent the formation of RCMκ-CN amyloid fibrils over the period of spectral acquisition.[37] For real-time NMR experiments, samples were incubated at 37 °C and spectra were recorded every 5 min. Each spectrum in the array was processed equally, and the resonance decay was calculated as a percentage of the absolute resonance intensity at 0 min. Random noise was of the order of 10% and was reduced to show overall trends using second-order Savitzky–Golay smoothing (15 neighbours). All spectra were referenced to the chemical shift of the HOD resonance and were processed using VNMRJ 2.1b software (Varian).

Pheochromocytoma-12 cell culture and MTT assay

PC12 cells were grown in RPMI 1640 medium supplemented with 10% v/v horse serum, 5% v/v foetal bovine serum, 10 U mL^{-1} of penicillin and 10 μg mL^{-1} of streptomycin. Cells were cultured in uncoated 75-cm^2 plastic flasks in an incubator with 95% air and 5% CO_2 at 37 °C. The medium was refreshed every 2–3 days. For treatment, cells from culture were seeded in 96-well plates at a density of 2×10^4 cells per well in 100-μL full-serum medium and then incubated for 24 h. The plated cells were then treated (six replicates per treatment) by diluting the incubated samples from the *in situ* ThT fluorescence assay directly into the cell culture medium to give a final RCMκ-CN concentration of 0.5 μM and/or the indicated concentrations of EGCG. The presence of residual ThT (0.1 μM) did not affect cell survival (data not shown). Recent unpublished work from our laboratory has shown that an RCMκ-CN concentration of 0.5 μM is most practicable for inducing cell death (F.C.D. *et al.*, unpublished data). Moreover, by first allowing for the formation of amyloid fibrils or inhibition thereof in a controlled environment *in vitro*, we avoid interference by active molecular chaperones, such as clusterin and BSA, which are readily present as nutrients in cell medium.[44,64,65] After incubation of the treated cells for 48 h, the treatment mixture was removed and 100 μL of serum-free medium containing MTT (0.6 mM) was added to each well. The cells were then incubated for an additional 2 h, and the MTT-containing medium was replaced with 100 μL of DMSO. Formazan absorption was then measured at 560 nm using a BMG Polarstar microplate reader (BMG Labtechnologies, Offenburg, Germany). Mean absorption readings from sextuplet wells were taken, and the percentage of MTT reduction (%) for each treatment was calculated using the following equation: MTT Reduction = A(treated)/A(untreated)×100, where A(treated) is the mean formazan absorption reading for each treatment and A(untreated) is the mean formazan absorption reading for cells treated with phosphate buffer only.

Statistics, smoothing and curve fitting

All tests of statistical significance, smoothing functions and curve fitting were performed using GraphPad PRISM 5.01 (GraphPad Software, San Diego, CA, USA).

Acknowledgements

This work was supported by a grant from the Australian Research Council to J.A.C. H.E. was supported by a National Health and Medical Research Council Peter Doherty Australian Biomedical Fellowship. We thank Lyn Waterhouse (Adelaide Microscopy, The University of Adelaide) for assisting with TEM and Phil Clements (School of Chemistry & Physics, The University of Adelaide) for assisting with the NMR experiments. We also gratefully acknowledge Dr. Kristen Bremmell (School of Pharmacy and Medical Sciences, University of South Australia) for helping with DLS measurements and Dr. Deborah Tew (Department of Pathology, The University of Melbourne) for kindly helping with the CD experiments.

Supplementary Data

Supplementary data associated with this article can be found, in the online version, at doi:10.1016/j.jmb.2009.07.031

References

1. Chiti, F. & Dobson, C. M. (2006). Protein misfolding, functional amyloid, and human disease. *Annu. Rev. Biochem.* **75**, 333–366.
2. Ecroyd, H. & Carver, J. A. (2008). Unraveling the mysteries of protein folding and misfolding. *IUBMB Life*, **60**, 769–774.
3. Westermark, P., Benson, M. D., Buxbaum, J. N., Cohen, A. S., Frangione, B., Ikeda, S. *et al.* (2005). Amyloid: toward terminology clarification. Report from the Nomenclature Committee of the International Society of Amyloidosis. *Amyloid*, **12**, 1–4.

4. Sacchettini, J. C. & Kelly, J. W. (2002). Therapeutic strategies for human amyloid diseases. *Nat. Rev. Drug Discov.* **1**, 267–275.
5. Rochet, J. C. (2007). Novel therapeutic strategies for the treatment of protein-misfolding diseases. *Expert Rev. Mol. Med.* **9**, 1–34.
6. Chaudhuri, T. K. & Paul, S. (2006). Protein-misfolding diseases and chaperone-based therapeutic approaches. *FEBS J.* **273**, 1331–1349.
7. Sciarretta, K. L., Gordon, D. J. & Meredith, S. C. (2006). Peptide-based inhibitors of amyloid assembly. *Methods Enzymol.* **413**, 273–312.
8. Porat, Y., Abramowitz, A. & Gazit, E. (2006). Inhibition of amyloid fibril formation by polyphenols: structural similarity and aromatic interactions as a common inhibition mechanism. *Chem. Biol. Drug Des.* **67**, 27–37.
9. Yamin, G., Ono, K., Inayathullah, M. & Teplow, D. B. (2008). Amyloid beta-protein assembly as a therapeutic target of Alzheimer's disease. *Curr. Pharm. Des.* **14**, 3231–3246.
10. Ono, K., Hirohata, M. & Yamada, M. (2008). Alpha-synuclein assembly as a therapeutic target of Parkinson's disease and related disorders. *Curr. Pharm. Des.* **14**, 3247–3266.
11. Barten, D. M. & Albright, C. F. (2008). Therapeutic strategies for Alzheimer's disease. *Mol. Neurobiol.* **37**, 171–186.
12. Dobson, C. M. (2006). Protein aggregation and its consequences for human disease. *Prot. Peptide Lett.* **13**, 219–227.
13. Riviere, C., Richard, T., Quentin, L., Krisa, S., Merillon, J. M. & Monti, J. P. (2007). Inhibitory activity of stilbenes on Alzheimer's beta-amyloid fibrils *in vitro*. *Bioorg. Med. Chem.* **15**, 1160–1167.
14. Kim, H., Park, B. S., Lee, K. G., Choi, C. Y., Jang, S. S., Kim, Y. H. & Lee, S. E. (2005). Effects of naturally occurring compounds on fibril formation and oxidative stress of beta-amyloid. *J. Agric. Food Chem.* **53**, 8537–8541.
15. Chen, D., Milacic, V., Chen, M. S., Wan, S. B., Lam, W.H., Huo, C. *et al.* (2008). Tea polyphenols, their biological effects and potential molecular targets. *Histol. Histopathol.* **23**, 487–496.
16. Basu, A. & Lucas, E. A. (2007). Mechanisms and effects of green tea on cardiovascular health. *Nutr. Rev.* **65**, 361–375.
17. Moon, H. S., Lee, H. G., Choi, Y. J., Kim, T. G. & Cho, C. S. (2007). Proposed mechanisms of (−)-epigallocatechin-3-gallate for anti-obesity. *Chem.-Biol. Interact.* **167**, 85–98.
18. Tipoe, G. L., Leung, T. M., Hung, M. W. & Fung, M. L. (2007). Green tea polyphenols as an anti-oxidant and anti-inflammatory agent for cardiovascular protection. *Cardiovasc. Hematol. Disord. Drug Targets*, **7**, 135–144.
19. Wolfram, S. (2007). Effects of green tea and EGCG on cardiovascular and metabolic health. *J. Am. Coll. Nutr.* **26**, 373S–388S.
20. Babu, P. V. & Liu, D. (2008). Green tea catechins and cardiovascular health: an update. *Curr. Med. Chem.* **15**, 1840–1850.
21. Khan, N. & Mukhtar, H. (2008). Multitargeted therapy of cancer by green tea polyphenols. *Cancer Lett.* **269**, 269–280.
22. Kim, J. A. (2008). Mechanisms underlying beneficial health effects of tea catechins to improve insulin resistance and endothelial dysfunction. *Endocr. Metab. Immune Disord. Drug Targets*, **8**, 82–88.
23. Yang, C. S., Ju, J., Lu, G., Xiao, H., Hao, X., Sang, S. & Lambert, J. D. (2008). Cancer prevention by tea and tea polyphenols. *Asia Pac. J. Clin. Nutr.* **17**(Suppl. 1), 245–248.
24. Yang, C. S., Lambert, J. D. & Sang, S. (2009). Antioxidative and anti-carcinogenic activities of tea polyphenols. *Arch. Toxicol.* **83**, 11–21.
25. Ono, K., Condron, M. M., Ho, L., Wang, J., Zhao, W., Pasinetti, G. M. & Teplow, D. B. (2008). Effects of grape seed-derived polyphenols on amyloid beta-protein self-assembly and cytotoxicity. *J. Biol. Chem.* **283**, 32176–32187.
26. Rezai-Zadeh, K., Arendash, G. W., Hou, H., Fernandez, F., Jensen, M., Runfeldt, M. *et al.* (2008). Green tea epigallocatechin-3-gallate (EGCG) reduces beta-amyloid mediated cognitive impairment and modulates tau pathology in Alzheimer transgenic mice. *Brain Res.* **1214**, 177–187.
27. Rasoolijazi, H., Joghataie, M. T., Roghani, M. & Nobakht, M. (2007). The beneficial effect of (−)-epigallocatechin-3-gallate in an experimental model of Alzheimer's disease in rat: a behavioral analysis. *Iran. Biomed. J.* **11**, 237–243.
28. Lin, C. L., Chen, T. F., Chiu, M. J., Way, T. D. & Lin, J.K. (2009). Epigallocatechin gallate (EGCG) suppresses beta-amyloid-induced neurotoxicity through inhibiting c-Abl/FE65 nuclear translocation and GSK3 beta activation. *Neurobiol. Aging*, **30**, 81–92.
29. Shimmyo, Y., Kihara, T., Akaike, A., Niidome, T. & Sugimoto, H. (2008). Epigallocatechin-3-gallate and curcumin suppress amyloid beta-induced beta-site APP cleaving enzyme-1 upregulation. *NeuroReport*, **19**, 1329–1333.
30. Mandel, S. A., Amit, T., Kalfon, L., Reznichenko, L., Weinreb, O. & Youdim, M. B. (2008). Cell signaling pathways and iron chelation in the neurorestorative activity of green tea polyphenols: special reference to epigallocatechin gallate (EGCG). *J. Alzheimer's Dis.* **15**, 211–222.
31. Avramovich-Tirosh, Y., Reznichenko, L., Mit, T., Zheng, H., Fridkin, M., Weinreb, O. *et al.* (2007). Neurorescue activity, APP regulation and amyloid-beta peptide reduction by novel multi-functional brain permeable iron- chelating- antioxidants, M-30 and green tea polyphenol, EGCG. *Curr. Alzheimer Res.* **4**, 403–411.
32. Choi, Y. T., Jung, C. H., Lee, S. R., Bae, J. H., Baek, W.K., Suh, M. H. *et al.* (2001). The green tea polyphenol (−)-epigallocatechin gallate attenuates beta-amyloid-induced neurotoxicity in cultured hippocampal neurons. *Life Sci.* **70**, 603–614.
33. Reznichenko, L., Amit, T., Zheng, H., Avramovich-Tirosh, Y., Youdim, M. B., Weinreb, O. & Mandel, S. (2006). Reduction of iron-regulated amyloid precursor protein and beta-amyloid peptide by (−)-epigallocatechin-3-gallate in cell cultures: implications for iron chelation in Alzheimer's disease. *J. Neurochem.* **97**, 527–536.
34. Ehrnhoefer, D. E., Bieschke, J., Boeddrich, A., Herbst, M., Masino, L., Lurz, R. *et al.* (2008). EGCG redirects amyloidogenic polypeptides into unstructured, off-pathway oligomers. *Nat. Struct. Mol. Biol.* **15**, 558–566.
35. Ehrnhoefer, D. E., Duennwald, M., Markovic, P., Wacker, J. L., Engemann, S., Roark, M. *et al.* (2006). Green tea (−)-epigallocatechin-gallate modulates early events in huntingtin misfolding and reduces toxicity in Huntington's disease models. *Hum. Mol. Genet.* **15**, 2743–2751.

36. Ecroyd, H., Koudelka, T., Thorn, D. C., Williams, D.M., Devlin, G., Hoffmann, P. & Carver, J. A. (2008). Dissociation from the oligomeric state is the rate-limiting step in fibril formation by kappa-casein. *J. Biol. Chem.* **283**, 9012–9022.
37. Thorn, D. C., Meehan, S., Sunde, M., Rekas, A., Gras, S. L., MacPhee, C. E. *et al.* (2005). Amyloid fibril formation by bovine milk kappa-casein and its inhibition by the molecular chaperones alphaS- and beta-casein. *Biochemistry*, **44**, 17027–17036.
38. Vreeman, H. J., Brinkhuis, J. A. & van der Spek, C. A. (1981). Some association properties of bovine SH-kappa-casein. *Biophys. Chem.* **14**, 185–193.
39. Kumosinski, T. F., Brown, E. M. & Farrell, H. M., Jr (1993). Three-dimensional molecular modeling of bovine caseins: a refined, energy-minimized kappa-casein structure. *J. Dairy Sci.* **76**, 2507–2520.
40. Farrell, H. M., Jr, Cooke, P. H., Wickham, E. D., Piotrowski, E. G. & Hoagland, P. D. (2003). Environmental influences on bovine kappa-casein: reduction and conversion to fibrillar (amyloid) structures. *J. Protein Chem.* **22**, 259–273.
41. Schmitz, K. S. (1990). *Dynamic Light Scattering By Macromolecules.* Academic Press, Boston, MA.
42. Paz, M. A., Fluckiger, R., Boak, A., Kagan, H. M. & Gallop, P. M. (1991). Specific detection of quinoproteins by redox-cycling staining. *J. Biol. Chem.* **266**, 689–692.
43. Gutierrez, P. L. (2000). The metabolism of quinone-containing alkylating agents: free radical production and measurement. *Front. Biosci.* **5**, D629–D638.
44. Marini, I., Moschini, R., Corso, A. D. & Mura, U. (2005). Chaperone-like features of bovine serum albumin: a comparison with alpha-crystallin. *Cell. Mol. Life Sci.* **62**, 3092–3099.
45. Zunszain, P. A., Ghuman, J., Komatsu, T., Tsuchida, E. & Curry, S. (2003). Crystal structural analysis of human serum albumin complexed with hemin and fatty acid. *BMC Struct. Biol.* **3**, 6.
46. Huo, C., Wan, S. B., Lam, W. H., Li, L., Wang, Z., Landis-Piwowar, K. R. *et al.* (2008). The challenge of developing green tea polyphenols as therapeutic agents. *Inflammopharmacology*, **16**, 248–252.
47. Kajiya, K., Kumazawa, S., Naito, A. & Nakayama, T. (2008). Solid-state NMR analysis of the orientation and dynamics of epigallocatechin gallate, a green tea polyphenol, incorporated into lipid bilayers. *Magn. Reson. Chem.* **46**, 174–177.
48. Feng, B. Y., Toyama, B. H., Wille, H., Colby, D. W., Collins, S. R., May, B. C. *et al.* (2008). Small-molecule aggregates inhibit amyloid polymerization. *Nat. Chem. Biol.* **4**, 197–199.
49. Weber, K. & Osborn, M. (1969). The reliability of molecular weight determinations by dodecyl sulfate-polyacrylamide gel electrophoresis. *J. Biol. Chem.* **244**, 4406–4412.
50. Meehan, S., Knowles, T. P., Baldwin, A. J., Smith, J. F., Squires, A. M., Clements, P. *et al.* (2007). Characterisation of amyloid fibril formation by small heat-shock chaperone proteins human alphaA-, alphaB- and R120G alphaB-crystallins. *J. Mol. Biol.* **372**, 470–484.
51. Rekas, A., Adda, C. G., Andrew Aquilina, J., Barnham, K. J., Sunde, M., Galatis, D. *et al.* (2004). Interaction of the molecular chaperone alphaB-crystallin with alpha-synuclein: effects on amyloid fibril formation and chaperone activity. *J. Mol. Biol.* **340**, 1167–1183.
52. Ecroyd, H. & Carver, J. A. (2009). Crystallin proteins and amyloid fibrils. *Cell. Mol. Life Sci.* **66**, 62–81.
53. Gazit, E. (2002). A possible role for pi-stacking in the self-assembly of amyloid fibrils. *FASEB J.* **16**, 77–83.
54. Gazit, E. (2005). Mechanisms of amyloid fibril self-assembly and inhibition. Model short peptides as a key research tool. *FEBS J.* **272**, 5971–5978.
55. Shoval, H., Lichtenberg, D. & Gazit, E. (2007). The molecular mechanisms of the anti-amyloid effects of phenols. *Amyloid*, **14**, 73–87.
56. Soto, C. & Estrada, L. D. (2008). Protein misfolding and neurodegeneration. *Arch. Neurol.* **65**, 184–189.
57. Stefani, M. & Dobson, C. M. (2003). Protein aggregation and aggregate toxicity: new insights into protein folding, misfolding diseases and biological evolution. *J. Mol. Med.* **81**, 678–699.
58. Shankar, G. M., Li, S., Mehta, T. H., Garcia-Munoz, A., Shepardson, N. E., Smith, I. *et al.* (2008). Amyloid-beta protein dimers isolated directly from Alzheimer's brains impair synaptic plasticity and memory. *Nat. Med.* **14**, 837–842.
59. Shechter, Y., Patchornik, A. & Burstein, Y. (1973). Selective reduction of cystine I–VIII in alpha-lactalbumin of bovine milk. *Biochemistry*, **12**, 3407–3413.
60. Fox, P. F. & McSweeney, P. L. H. (1998). *Dairy Chemistry and Biochemistry.* Blackie Academic & Professional, London, UK.
61. Peters, T., Jr. (1995). *All About Albumin: Biochemistry, Genetics, and Medical Applications.* Academic Press Inc., San Diego, CA.
62. Provencher, S. W. (1982). CONTIN: a general purpose constrained regularization program for inverting noisy linear algebraic and integral equations. *Comput. Phys. Commun.* **27**, 229–242.
63. Koppel, D. E. (1972). Analysis of macromolecular polydispersity in intensity correlation spectroscopy: the method of cumulants. *J. Chem. Phys.* **57**, 4814–4820.
64. Yerbury, J. J., Poon, S., Meehan, S., Thompson, B., Kumita, J. R., Dobson, C. M. & Wilson, M. R. (2007). The extracellular chaperone clusterin influences amyloid formation and toxicity by interacting with prefibrillar structures. *FASEB J.* **21**, 2312–2322.
65. Maiti, T. K., Ghosh, K. S. & Dasgupta, S. (2006). Interaction of (−)-epigallocatechin-3-gallate with human serum albumin: fluorescence, Fourier transform infrared, circular dichroism, and docking studies. *Proteins*, **64**, 355–362.